

LOW CYCLE FATIGUE BEHAVIOURS OF THE WELDED JOINTS OF 9 TO 12 % CR FERRITIC HEAT RESISTANT STEELS FOR BOILER OF FOSSIL POWER PLANTS

Seog-Hyeon Ryu, Yeon-Soo Lee, Byeong-Ook Kong and Jeong-Tae Kim
Materials Evaluation and Development Team, Corporate R&D Institute
DOOSAN Heavy Industries & Construction Co. Ltd
555 Gwigok-dong, Changwon, Gyeongnam 641-792, Korea

Dong-Ho Kwak and Soo-Woo Nam
Korea Advanced Institute of Science and Technology
373-1 Guseong-Dong, Yuseong-Gu, Daejeon 305-701, Korea

ABSTRACT

Behaviours of continuous LCF and CFI with 10 minute hold time have been investigated at temperature range from 550 °C to 700 °C in P92 and P122 pipe steels. Specimens were prepared from the base metal, the HAZ, and the weld metal of the welded joints fabricated by SMAW process. Additionally, effects of delta-ferrite on fatigue life have been investigated in P92 with approximate 8% delta-ferrite stringer.

A typical cyclic softening behaviour was observed in all positions of welded joints of P92 and P122 pipe steels during continuous LCF and CFI tests. The continuous LCF life of P122 was slightly higher than that of P92 over test conditions studied. The superiority of P122 on P92 in continuous LCF is attributed to its higher yield strength relatively. The CFI life in the HAZ and the weld metal of P122 caused a reduction in cycles to failure by the factor of 2 to 4 than that of the continuous LCF. The dissolution of very fine Cu-rich precipitates and the reprecipitation as coarse particles during welding and PWHT caused the reduced CFI life in the HAZ of P122. Approximate 8% delta-ferrite resulted in the reduction of continuous LCF life by the factor of 2 as fatigue loading was perpendicular to delta-ferrite stringer.

KEYWORDS

Low Cycle Fatigue (LCF), Creep-fatigue interaction (CFI), P92, P122, VM12, Heat Affected Zone (HAZ), Delta-ferrite, Ferritic Heat Resistant Steels.

INTRODUCTION

To increase efficiency and reduce CO₂ emissions, there has been a drive to increase operating temperatures and pressures of fossil power plants since 1990's. Higher steam pressure and steam temperatures call for superior strength materials. Therefore, materials selection for thick-section components of boiler systems should be determined by considering creep rupture strength and thermal fatigue resistance as well as fabricability and weldability.

Ferritic steels are usually preferred for these working conditions due to higher thermal properties and fatigue strength than those of austenitic steels. Among 9 to 12 % Cr ferritic steels, P92, P122, and VM12 pipe steels with higher allowable stress result in reduced wall thickness [1] [2]. Reduced

wall thickness enables reduced thermal fatigue damage, increased life of critical components, and two shift start-up and shut-down.

Boiler materials such as pipe and tubing have been applied to the components by means of welding and bending processes. Generally, from a microstructural viewpoint, the welded joint is composed of the base metal, the heat affected zone (HAZ), and the weld metal. Therefore, significant variations in the fracture behaviours exist across the welded joint. Especially, for the thick-walled components, a reasonable assessment of cyclic damage at high temperatures is an important issue for the current power plants operating with frequent start-up and shut-down mode.

In this study, behaviours of continuous LCF (Low Cycle Fatigue) and CFI (Creep-Fatigue Interaction) with 10 minutes hold time at temperature range from 550 °C to 700 °C have been investigated in the base metal, the HAZ, and the weld metal of weldment fabricated by SMAW (Shielded Metal Arc Welding) process in P92 and P122. Additionally, effects of delta-ferrite on fatigue life have been investigated in P92. Continuous LCF and CFI tests were carried out for different loading directions, parallel and perpendicular to delta-ferrite stringer.

EXPERIMENTAL PRECEDURES

The chemical compositions of pipe steels studied and matching welding electrodes are given in Table 1. The dimensions of pipes are OD (Outside Diameter) 304 mm and WT (Wall Thickness) 62 mm for P92, OD 395 mm and WT 50 mm for P122, and OD 406 mm and WT 35 mm for VM12. The microstructure of the as-received materials consisted of matrix of tempered martensite and small fractions of delta ferrite less than about 1 volume percent in all pipe steels except in P92 (II) steel, which contained approximate 8 percent delta-ferrite. Table 2 shows the mechanical properties of the as-received materials for P92, P122, and VM12 steels. The welding processes used in the study consisted of GTAW (Gas Tungsten Arc Welding), which was employed for the root pass welding, and SMAW. The PWHT (Post Welding Heat Treatment) was carried out at 760 °C for 5 hours. The details of the welding parameters are shown in Table 3. No defects were observed in the weld metal and the HAZ. Microstructures of the weld metal for all pipe steels were tempered martensitic structures with a small content of delta ferrite less than one volume percent. Additionally, P122 contained retained austenite below about 4 % in the weld metal.

The tensile specimens with the gage section of 6.25 mm and 30 mm in diameter and length respectively were cut out across the circumferential weld seam for cross weld properties and at the weld seam for all weld metal properties. The full-sized 10 x 10 mm Charpy V-notch specimens were obtained across the circumferential weld seams. A V-notch was placed in the base metal, the HAZ, and the centre of weld deposit respectively. Tensile and impact tests were conducted at the room temperature of 20°C.

The specimens for LCF and CFI tests were machined at the three different locations across the circumferential weld seam. The three sampling locations included base metal, HAZ, and weld metal. The weld and base metal samples were composed only of weld deposit and base metal at the gage part respectively. While, the HAZ sample was comprised of the base metal, the HAZ, and the weld metal in gage part. The centre of the HAZ coincided with the middle of the gage length. The dimension of gage part of LCF and CFI test samples was 7 mm in diameter and 8 mm in length. For all LCF tests, uniaxial strain control push-pull tests were performed at a strain rate of $4 \times 10^{-3} \text{ s}^{-1}$ with total strain range from $\pm 1.0 \%$ to $\pm 3.0 \%$ with $\pm 0.5 \%$ intervals at normal atmospheric conditions. A symmetrical continuous triangular loading waveform was used for LCF test. Fatigue tests for the base metal, the HAZ and the weld metal were conducted at the

temperatures range from 550 °C to 700 °C with 50 °C intervals. CFI tests were performed with strain-hold of 10 minutes at tensile peak strain as the same temperature with LCF test.

Table 1. Chemical compositions of the as-received materials (base metals) and the matching welding electrodes for P92, P122, and VM12 steels.

Element	Base Metal				Welding Electrode for SMAW		
	P92 (I) ¹⁾	P92 (II) ¹⁾	P122 ²⁾	VM12 ¹⁾	P92 ³⁾	P122 ⁴⁾	VM12 ³⁾
C	0.10	0.09	0.13	0.12	0.11	0.08	0.12
Si	0.22	0.15	0.31	0.49	0.22	0.33	0.50
Mn	0.48	0.42	0.59	0.35	0.54	0.79	0.60
P	0.017	0.013	0.020	0.018	0.014	0.010	0.017
S	0.006	0.002	-	0.001	0.005	0.004	0.007
Ni	0.18	0.24	0.34	0.29	0.59	0.94	0.70
Cr	9.11	9.15	10.57	11.50	8.50	10.01	11.20
Mo	0.47	0.48	0.33	0.29	0.50	0.19	0.30
W	1.71	1.67	1.79	1.50	1.45	1.44	1.50
V	0.18	0.192	0.21	0.26	0.20	0.16	0.25
Nb	0.056	0.065	0.060	0.05	0.02	0.02	0.05
Cu	-	-	0.96	-	0.06	1.50	-
Co	-	-	-	1.62			1.60
B	0.003	0.0029	0.002	0.0049	0.002	0.002	0.0030
N	0.041	0.043	0.060	0.0665	0.041	0.039	0.060

1) and 2) were supplied by V&M Tubes Co. and Sumitomo Metal Industries, Ltd. respectively. 3) and 4) were supplied by Thyssen Krupp Stahlunion GMBH and Sumikin Welding Industries, Ltd. respectively.

Table 2. Dimensions and mechanical properties of the as-received materials.

Steel	Dimension (mm)	Heat treatment ¹⁾	Mechanical Properties			
			TS (MPa)	YS _{0.2%} (MPa)	EL (%)	HRB
P92	OD 304 x WT 62	N: 1050 °C x 1 hr, AC T: 760 °C x 3 hrs, AC	674	506	23.6	-
P122	OD 395 x WT 50	N: 1050 °C x 0.5 hrs, AC T: 770 °C x 6 hrs, AC	758	591	24	221
VM12	OD 406 x WT 35	N: 1060 °C x 0.5 hrs, AC T: 780 °C x 2 hrs, AC	792	608	22	-

1) N: Normalizing, T: Tempering, AC: Air cooling from austenitizing temperature.

Table 3. Welding Parameters for SMAW Process in P92, P122, and VM12 Steels

Parameters	Number
Welding Current	140~180 A
Welding Voltage	18~26
Travel Speed	4~15 cm/min
Preheat and Interpass Temperature	200-300 °C
Diameter of Electrode	4.0 mm
Heat Input	40~54 kJ/cm
Welding Pass	30
Post weld heat treatment	760 °C x 5 hrs

RESULTS AND DISCUSSION

Mechanical properties of the welded joints at room temperature

Fig.1 shows tensile properties of the cross weld and the weld metal after the PWHT at 760 °C for 5 hours in P92, P122, and VM12 steels. All cross weld samples were fractured at the base metal. As compared to the tensile strength of the as-received materials shown in Table 2, the cross weld tensile strengths were found to be somewhat higher. It seems that the higher tensile strengths in the cross weld samples were affected by the constrained effect caused by the hardened areas, such as the HAZ and the weld metal. The weld metal tensile strength was always superior to those of the base metal and cross weld in three pipe steels. The cross weld and weld metal tensile strengths of P122 and VM12 with higher chromium content were similar to each other over welding parameters studied and they were higher than that of P92 as expected from the as-received properties.

Charpy impact energy at room temperature is given in Fig.2. The base metal of P92, P122, and VM12 exhibits relatively lower toughness level compared with the low alloy steels due to adding elements such as chromium and tungsten. The problem related with the lower toughness is limited only to the weld metal and the HAZ region of the welded joint because the base metal toughness was restored to the extent of approximate 80~180 J/cm² after tempering at about 760 °C carried out at mill makers. As shown in Fig.2, the HAZ toughness was restored up to the similar or higher values compared to the base metal by the PWHT of 760°C for 5 hours in three pipe steels. The weld metal toughness was lower compared to the base metal and the HAZ. On the contrary of tensile properties, the weldment toughness of P92 was relatively superior to P122 and VM12 over welding conditions studied.

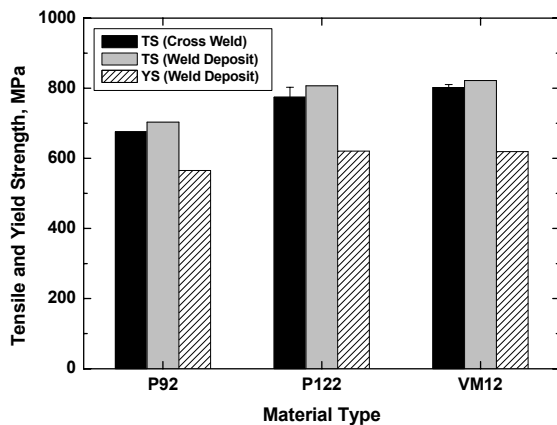


Fig.1 Tensile properties at room temperature of P92, P122, and VM12 pipe steels

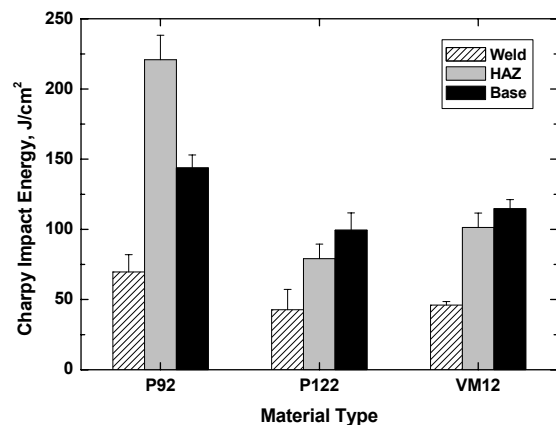


Fig.2 Charpy impact absorbed energy at room temperature of P92, P122, and VM12 pipe steels

Low Cycle Fatigue Properties

The typical cyclic softening behaviour occurred in the tempered martensitic structure was observed in the base metal, the HAZ, and the weld metal of P92 and P122 steels during the continuous LCF and CFI tests. Fig.3 shows the relationship of total strain range ($\Delta\epsilon_t$) versus the number of cycles to failure (N_f) for the base metal, the HAZ, and the weld metal under continuous LCF at temperature ranges from 550 °C to 700 °C with 50 °C intervals in P92 and P122. In Figures, lines represent best fit of experimental data points for the base metal and the HAZ.

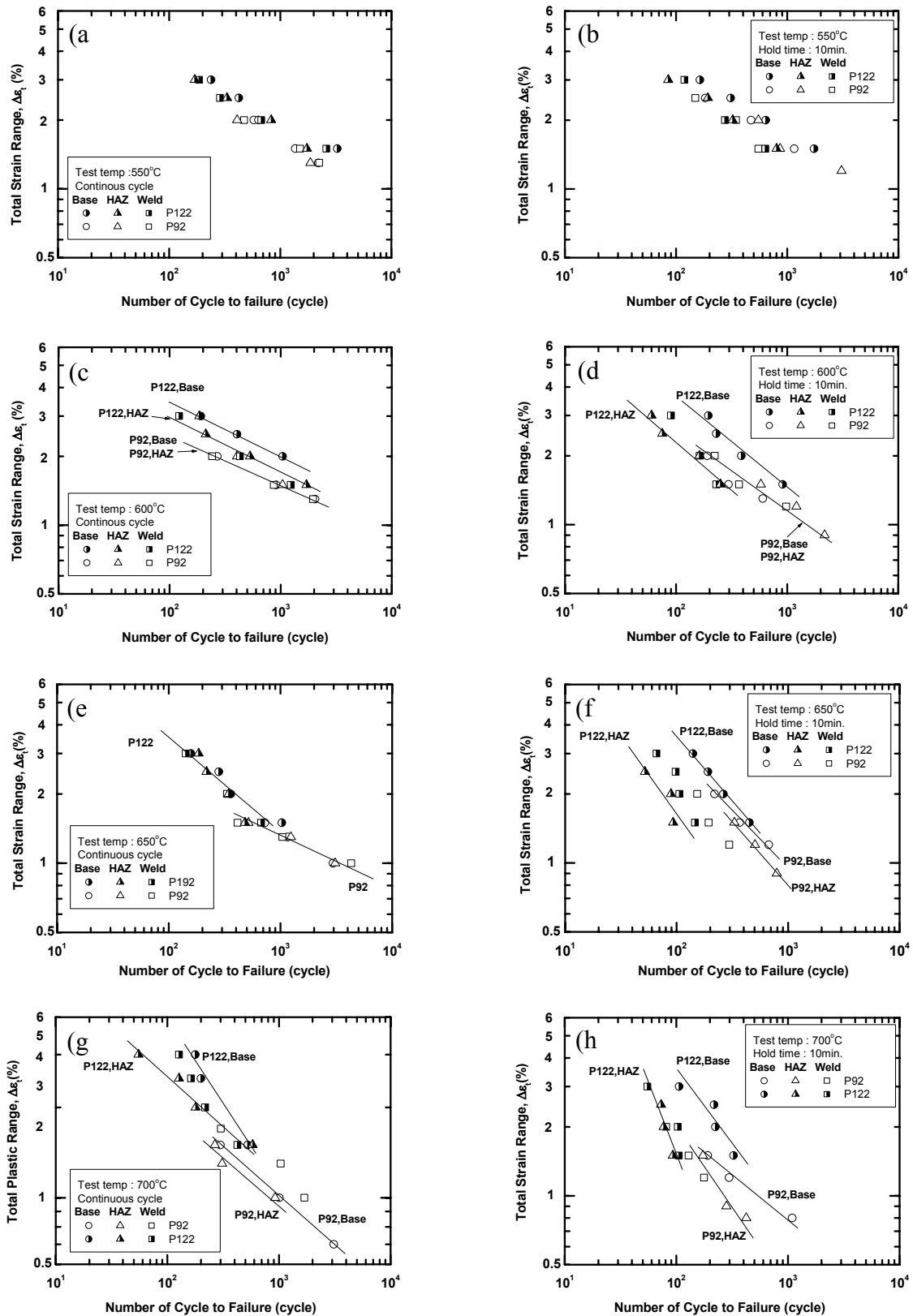


Fig.3 Comparison of fatigue life of the base metal, the HAZ, and the weld metal in P92 and P122 pipe steels. (a) (b) continuous LCF and CFI life at 550 °C respectively. (c) (d) continuous LCF and CFI life at 600 °C respectively. (e) (f) continuous LCF and CFI life at 650 °C respectively. (g) (h) continuous LCF and CFI life at 700 °C

At all testing temperatures, continuous LCF life of P122 was superior to that of P92 over test conditions studied although there was not remarkable difference in fatigue life. It is considered that the superiority of P122 on P92 in continuous LCF is attributed to its higher yield strength relatively and smaller plastic strain range at a fixed total strain range. At a given plastic strain range, the difference in continuous LCF life was negligible [3]. The continuous LCF lives for the base metal of P92 and P122 at 600 °C were similar to the results reported by M. Sato et al. [4].

The results of CFI tests with 10 minutes hold time are given in Fig.3 (b), (d), (f), and (h). In the base metal, the continuous LCF and CFI tests indicated nearly similar fatigue life regardless of the 10 minutes hold time. The CFI life in the weld metal and the HAZ of P122 caused a reduction in cycles to failure by the factor of 2 to 4 than that of the continuous LCF. The extent of reduction increased with increasing temperatures. In P92 steel, the reduction of the CFI life in the HAZ and the weld metal was not pronounced at 550 °C to 650 °C. However, at 700 °C and in lower total strain range of less than 0.8 %, the difference between the base metal and the HAZ is not negligible in even P92. Coffin-Manson plots describing the plastic strain amplitude versus fatigue life showed that the HAZs of P92 and P122 had degraded fatigue resistances for CFI compared to continuous LCF (Fig.4). Especially, the HAZ of P122 showed lower CFI life and higher CFI temperature dependence with slopes of range 0.6 to 0.9 according to temperature range from 550 °C to 700 °C in the Coffin-Manson plot.

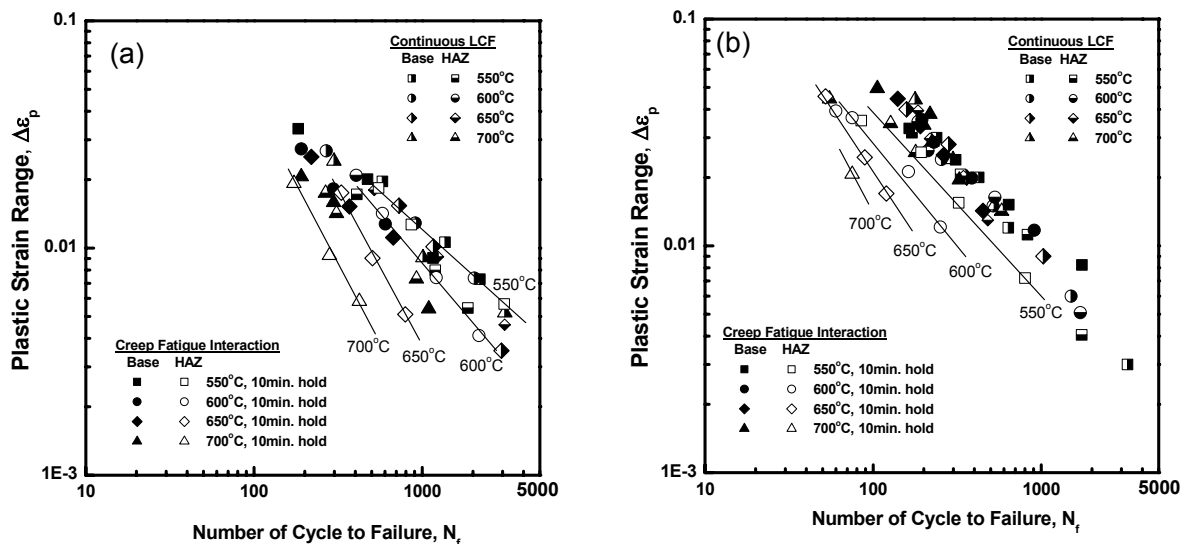


Fig.4 Coffin-Manson plots at temperatures 550 °C to 700 °C for the base metal and the HAZ of (a) P92 and (b) P122 pipe steels.

The fractured surfaces were examined by scanning electron microscopy as shown in Fig.5. All surfaces failed by fatigue crack initiation and propagation consisted of areas of heavily oxidized transgranular failure and fatigue striation formed perpendicular to the direction of fatigue crack growth. The striation spacing of the HAZ after CFI test (Fig.5 (c)) in P92 was larger than at the continuous LCF test (Fig.5 (b)) and agreed with fatigue life.

In a different way with continuous LCF, the reduction of CFI life in the HAZ and the weld metal means that hold time effect on the microstructural changes is severer in the weld metal and the HAZ than in the base metal. As comparing the microstructural evolutions developed in the weld metal and the HAZ to that in the base metal during CFI test, the recovery of lath structure and the formation of subgrain structure were produced seriously in the weld metal locally rather than in the

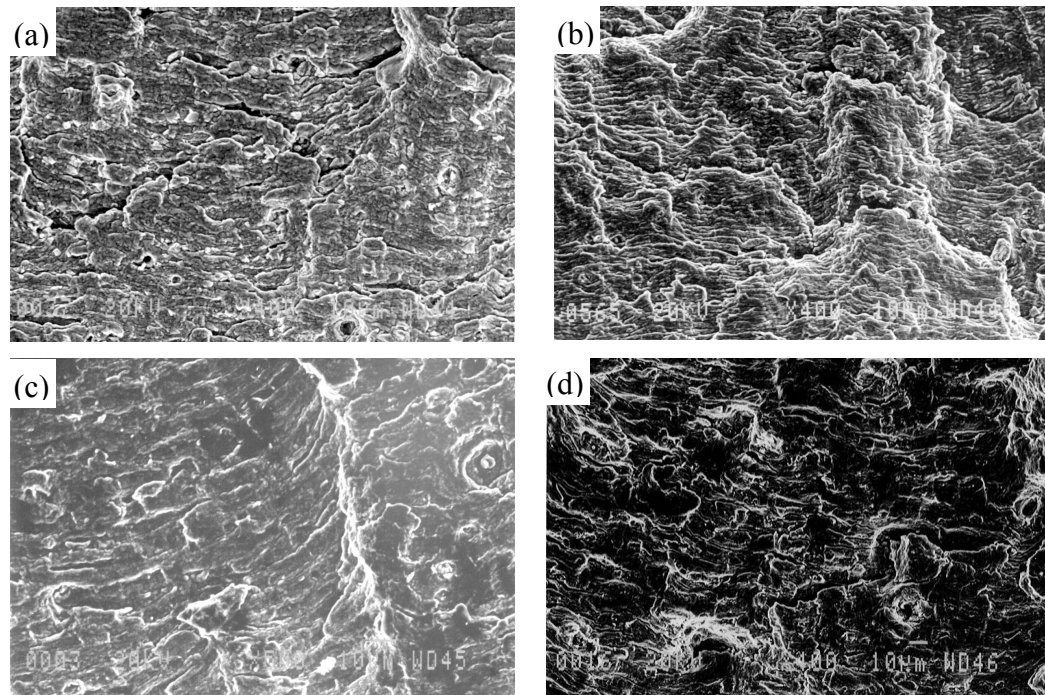


Fig.5 The appearance of fracture surface formed after continuous LCF and CFI tests at 650 °C with ± 1.5 % total strain range in P92 and P122 pipe steels. (a) P92-Base ($N_f = 727$), continuous LCF. (b) P92-HAZ ($N_f = 517$), continuous LCF. (c) P92-HAZ ($N_f = 330$), CFI. (d) P122-Base ($N_f = 1029$), continuous LCF.

base metal. It is considered that the local accelerated recovery and recrystallization results from the intrinsic non-homogeneity and the loose structure of the weld metal as compared to the base metal. Therefore, the additional microstructural evolutions caused by the creep deformation during the holding time offers the large plastic strain and leads to the decrease of fatigue life in the weld metal during the CFI test. In the study, the HAZ specimen is composed of the base metal, the HAZ and the weld metal at the gage part although the HAZ is placed in the centre of the gauge part. Fatigue cracks during LCF test could be initiated at the weld metal or the base metal as well as the HAZ. However, fatigue cracks were initiated at the HAZ region near to weld metal on 13 specimens among 15 pieces over test conditions studied. Fig.6 shows the difference of microstructural evolution represented in the base metal and the HAZ of P92 and P122 after fatigue test. The extent of microstructural evolution is associated with the recovery and sub-grain formation of dislocation structure and the nucleation and growth of fine precipitates. The microstructural change in the HAZ was more pronounced compared to the base metal. In the HAZ of P122 steel after CFI test, Cu-rich particle was observed abundantly in the matrix and grain boundaries compared to the base metal and the HAZ after continuous LCF test. Therefore, it might be concluded that the considerable reduction of CFI life in the HAZ is attributed to the dissolution of very fine Cu-rich precipitate and the reprecipitation as coarse particles during welding and PWHT.

Effect of Delta Ferrite on Low Cycle Fatigue Behaviours

The composition of P92 is carefully balanced to avoid delta ferrite formation. In weldment, a small amount of delta-ferrite less than about 5% indicates beneficial effects in reducing weld cracking. However, delta-ferrite is generally regarded as detrimental for toughness and long-term creep rupture strength. Additionally, delta-ferrite content greater than approximate 5% is considered to be lowering hot workability for pipe and tube making. The compositional range of P92 pipe steel

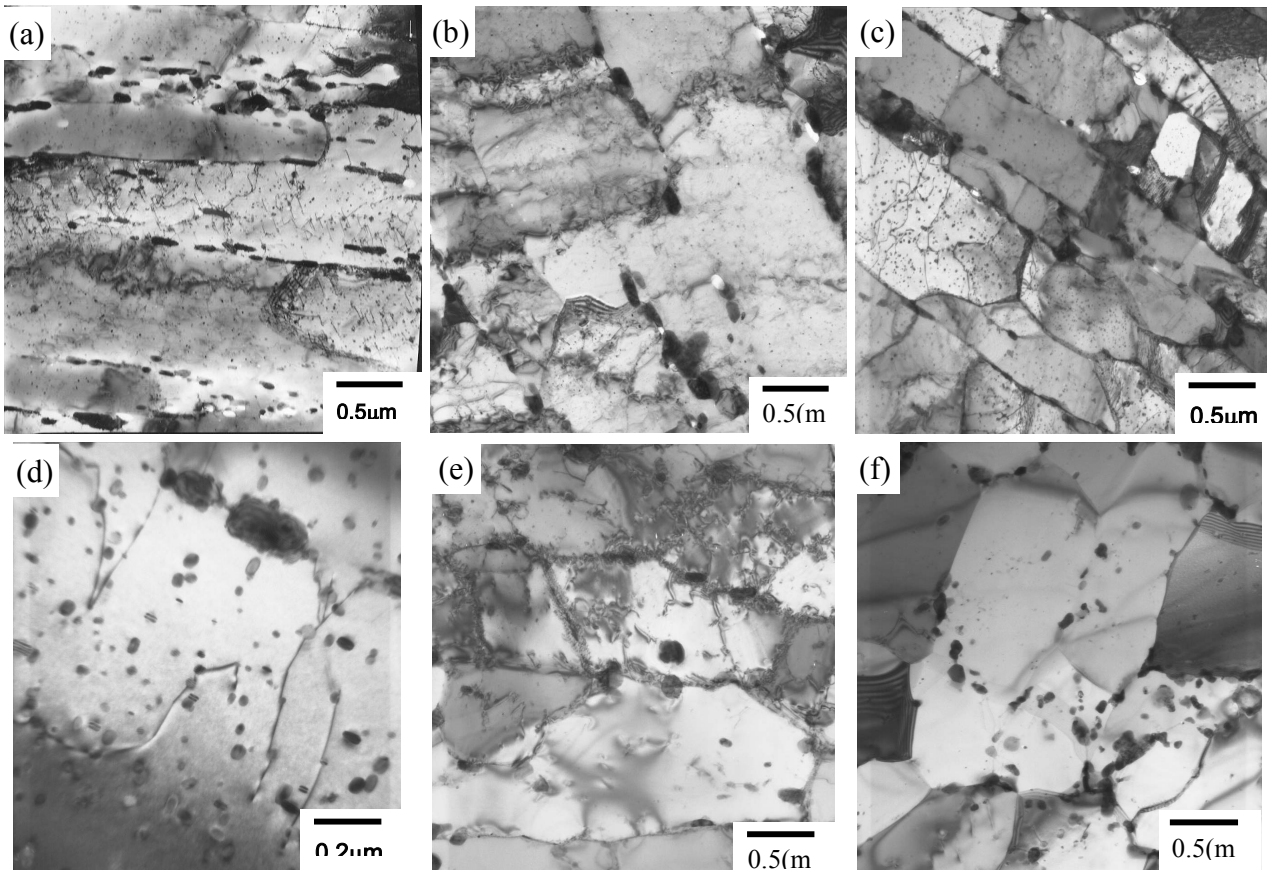


Fig.6 TEM Microstructures after continuous LCF and CFI tests at 650 °C with ± 1.5 % total strain range in P22 and P122 pipe steels. (a) P122-Base metal. (b) P122-HAZ ($N_f = 481$), continuous LCF. (c) P122-HAZ ($N_f = 93$), CFI. (d) Magnified microstructure of (c). (e) P92-HAZ ($N_f = 517$), continuous LCF. (f) P92-HAZ ($N_f = 330$), CFI.

specified in ASME SA-335 has the tendency for delta-ferrite formation in the conditions of special selection of alloying elements under the chemical composition of specification. According to S. H. Ryu et al. [5], 9 to 12 percent Cr ferritic steels with net chromium equivalent (net Cr_{eq}), which is proposed as $net\ Cr_{eq}\ (\%) = Cr + 0.8Si + 2Mo + 1W + 4V + 2Nb + 1.7Al + 60B + 2Ti + 1Ta - 2.0Ni - 0.4Mn - 0.6Co - 0.6Cu - 20N - 20C$, greater than 10 % contains delta-ferrite. P92 has net Cr_{eq} values range from 6.3 to 12.5. P92(I) and P92(II) shown in Table 1 has average net Cr_{eq} value of 9.6 and 9.7 respectively. Therefore, they should contain only fully tempered martensitic structure without delta-ferrite but approximate 8% delta-ferrite existed in P92 (II) of the as-received condition due to the local increase of net Cr_{eq} caused by local segregation or unknown factors.

Fig.7 (a) shows the microstructure composed of 8% delta-ferrite and matrix of tempered martensite in P92 (II). The direction of delta-ferrite stringer was parallel to the extrusion direction for pipe production. Stringer type of delta-ferrite was destroyed partially after induction bending followed by normalizing and tempering shown in Table 2 (Fig. 7 (b)).

The effect of delta-ferrite on fatigue life is given in Fig. 8. Continuous LCF and CFI tests carried out for different loading directions, parallel and perpendicular to delta-ferrite stringer. In case of loading parallel to stringer, 8% delta-ferrite had no effect on continuous LCF and CFI life at 600 °C and 650 °C compared to 0% delta-ferrite. On the contrary, as fatigue loading was acted on perpendicular to delta-ferrite stringer, 8 % delta-ferrite had a negative influence on fatigue life over test conditions studied. Therefore, as the stringer type delta-ferrite was formed within the matrix of tempered martensite, the difference of fatigue life varied with the loading direction.

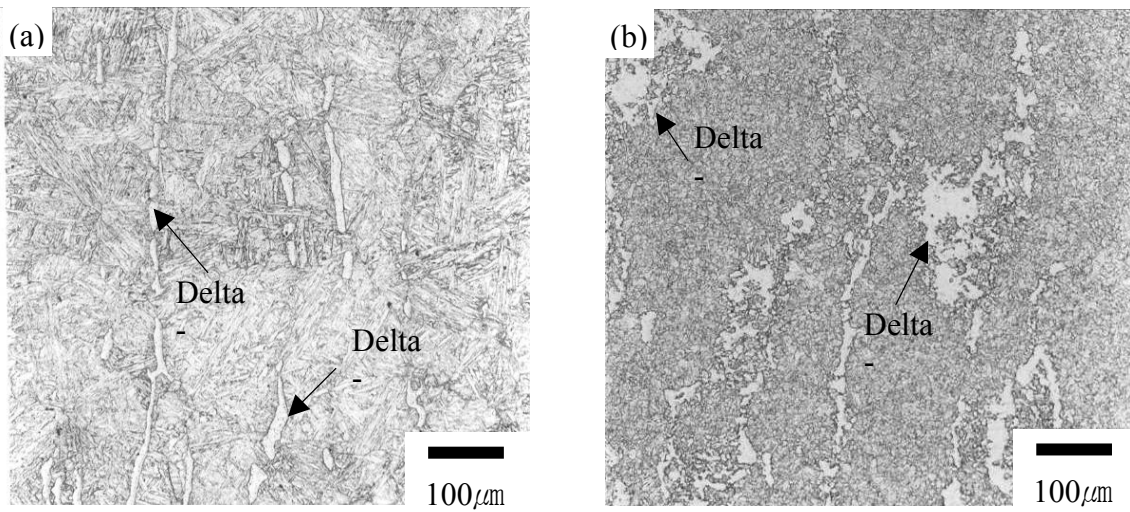


Fig.7 The size, shape and distribution of delta-ferrite within the matrix of tempered martensite. (a) The as-received material. (b) After induction bending followed by normalizing and tempering.

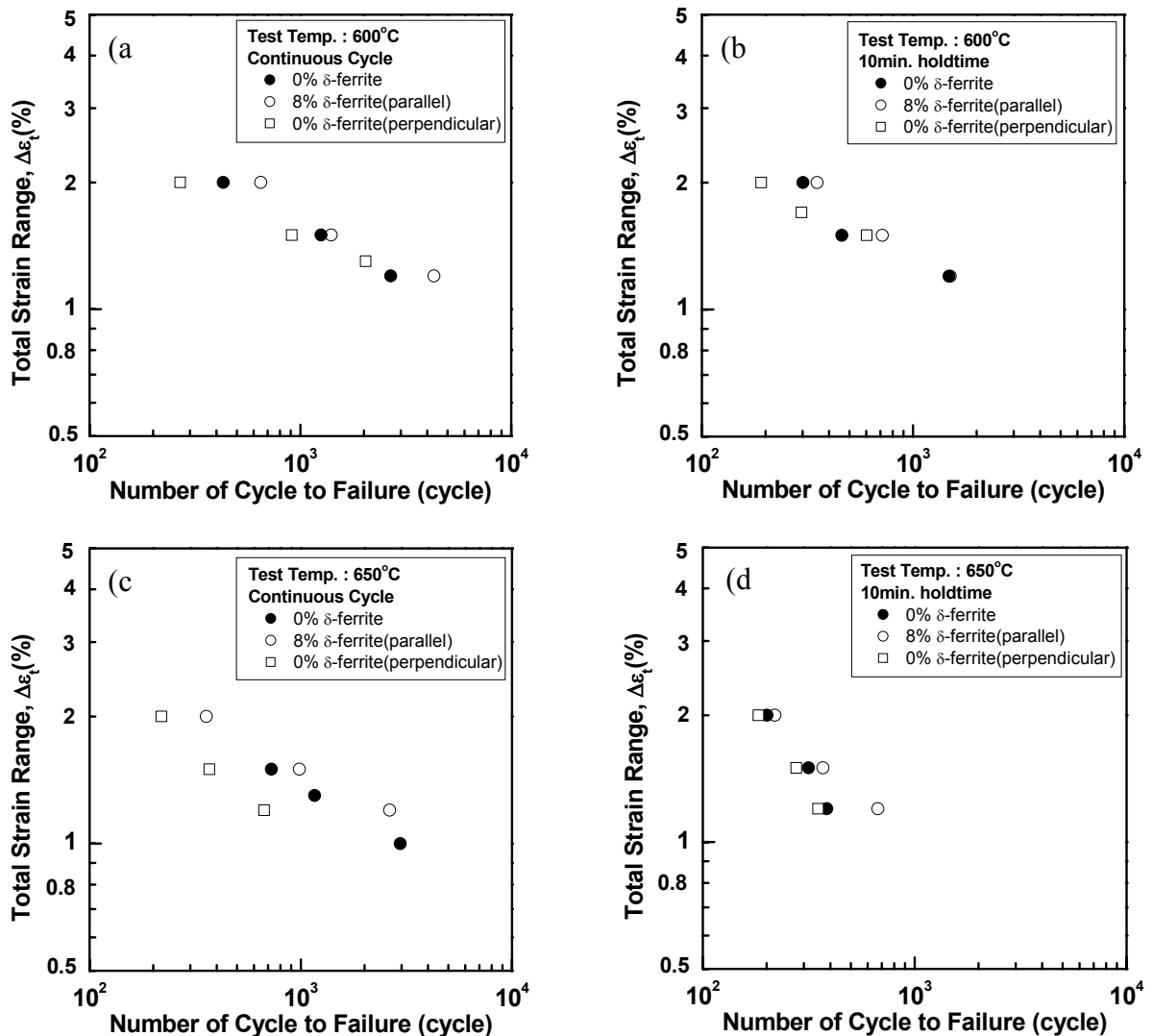


Fig.8 Variation of fatigue life of the base metal in P92 with the delta-ferrite content and the direction between stress axis and delta-ferrite stringer. (a) (b) continuous LCF and CFI life at 600 °C respectively. (c) (d) continuous LCF and CFI life at 650 °C respectively.

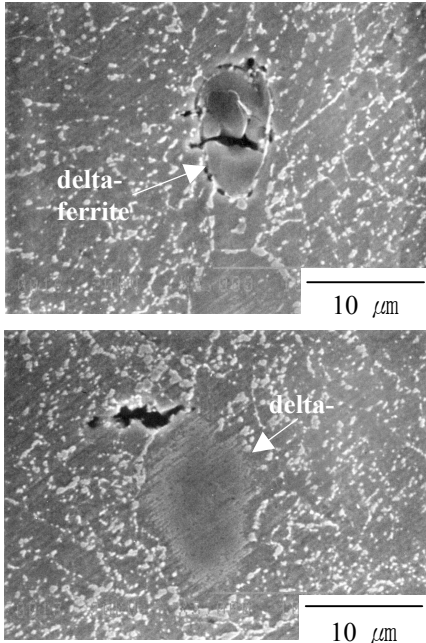


Fig.9 Crack initiation and propagation from the delta-ferrite or the delta-ferrite / matrix interface

Fig.9 shows effects of delta-ferrite on crack initiation and propagation as fatigue loading was parallel to delta-ferrite stringer. Fatigue crack was initiated from the crevice of the delta-ferrite within the matrix or the delta-ferrite/matrix interface as fatigue loading was parallel to delta-ferrite stringer. These types of crack initiation and propagation hardly influenced on fatigue life at 600 °C and 650 °C as shown in Fig. 8. As fatigue loading was perpendicular to delta-ferrite stringer, surface fatigue crack was initiated and propagated from the delta-ferrite or along the delta-ferrite/matrix interface as shown in Fig.10. It seems that the easy formation of surface cracks due to the presence of delta-ferrite stringer exposed at the surface reduces continuous LCF life as fatigue loading was perpendicular to delta-ferrite stringer.

E.A. Roria [6] reported that 5% delta-ferrite contained in 12% Cr steel contributed to the improvement of high cycle fatigue strength compared to 0% delta-ferrite. On the contrary, as the levels of delta-ferrite increased to about 15 to 20%, the fatigue strength decreased to 140 ksi compared to 150 ksi of 0% delta-ferrite. According to E. Krainer et al. [7], 5 to 10% delta-ferrite showed superior high cycle fatigue strength compared to the material without delta-ferrite in 12% Cr steel. However, in the study, continuous LCF life reduced by the factor of 2 by the presence of approximate 8% delta-ferrite as fatigue loading was perpendicular to delta-ferrite stringer.

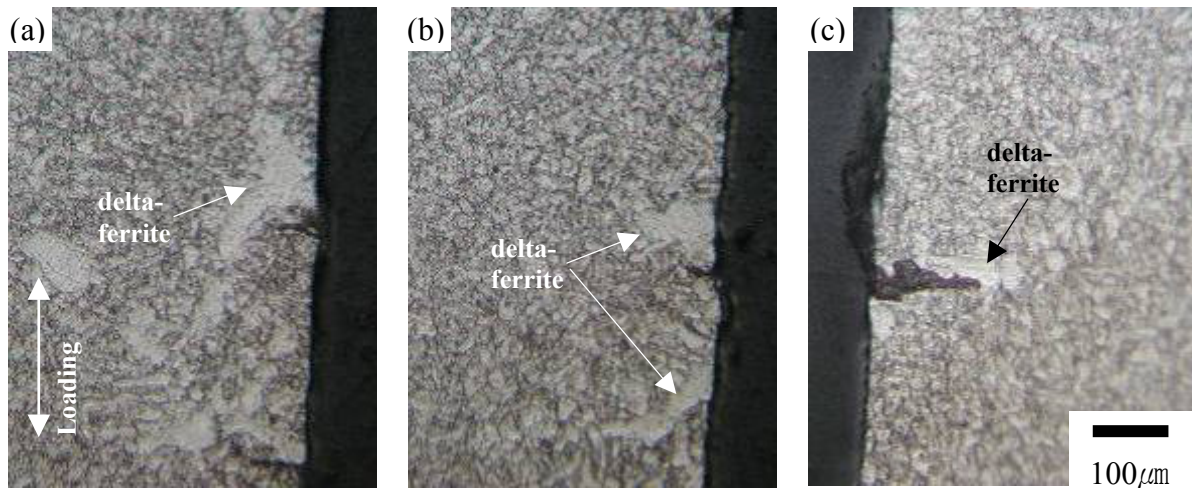


Fig.10 Surface crack initiation and propagation from the delta-ferrite or along the delta-ferrite/matrix interface in the case of loading perpendicular to delta-ferrite stringer.

CONCLUSION

A typical cyclic softening behaviour was observed in the base metal, the HAZ, and the weld metal of P92, P122 pipe steels during continuous LCF and CFI tests.

The continuous LCF life of P122 was superior to that of P92 over test conditions studied although there was not remarkable difference in fatigue life. The superiority of P122 on P92 in continuous LCF is attributed to its higher yield strength relatively.

The CFI life in the HAZ and the weld metal of P122 caused a reduction in cycles to failure by the factor of 2 to 4 than that of the continuous LCF. The dissolution of very fine Cu-rich precipitates and the reprecipitation as coarse particles during welding and PWHT caused the reduced CFI life in the HAZ. The extent of reduction increased with increasing temperatures.

Approximate 8% delta-ferrite resulted in the reduction of continuous LCF life by the factor of 2 as fatigue loading was perpendicular to delta-ferrite stringer. However, 8% delta-ferrite hardly influenced on continuous LCF and CFI lives as fatigue loading was parallel to delta-ferrite stringer.

The easy formation of surface cracks caused by the presence of delta-ferrite stringer exposed at the surface was associated with the reduction in continuous LCF life as fatigue loading was perpendicular to delta-ferrite stringer.

REFERENCES

- 1) ASME Boiler & Pressure Vessel Code An International Code, Section II, Part D, 2004 Edition, July 1, 2004, The American Society of Mechanical Engineers.
- 2) J. Gabrel, W. Bendick, J.C. Vaillant, B. Vandenberghe, and Bo. Lefebvre, Proc. 4th Int. Conf. on Advances in Materials Technology for Fossil Power Plants, Oct.25-28, 2004, Hilton Head Island, South Carolina, p.919.
- 3) S.H. Ryu et al., Proc. of the 7th Liège Conf. on Materials for Advanced Power Engineering 2002, Part III, Liège, Belgium, 2002, pp.1681-1690.
- 4) M. Sato et al., Proc. on Advanced Heat Resistant Steels for Power Generation, San Sebastian, Spain, 1998, pp.298-308.
- 5) S.H. Ryu and J. Yu, Metall. and Mat. Trans. A, Vol. 29A, June 1998, p.1573.
- 6) E.A. Loria, Influence of Delta Ferrite-Carbide Segregates on the Properties of 12% Chromium Steel, Trans. ASM 54, (1961), S.31-49, S.705.
- 7) E. Krainer, Kapfenberg, and H. Scheidl, Radex-Rundschu, 1977, Heft 3, pp. 246.